MOLECULAR PHYSICS, 20 JULY–10 AUGUST 2004, VOL. 102, NO. 14–15, 1615–1623

Taylor & Francis
Taylor & Francis Group

Determination of the excited state structure of 7-azaindole using a Franck–Condon analysis

ROBERT BRAUSE, MICHAEL SCHMITT*, DANIEL KRÜGLER†
and KARL KLEINERMANNS*

Heinrich-Heine-Universität, Institut für Physikalische Chemie, D-40225 Düsseldorf, Germany

(*Received 1 March 2004; revised version accepted 26 March 2004*)

The change in structure of 7-azaindole upon electronic excitation was determined by a Franck–Condon analysis of the intensities in the fluorescence emission spectra obtained via excitation of six different vibronic bands. A total of 107 emission band intensities were fit, together with the changes in the rotational constants of four 7-azaindole isotopomers. The geometry change of the ring framework upon electronic excitation from the electronic ground state to the ^1L_b state ($\pi\pi^*$) can be described by an overall expansion of the pyridine ring of 7-azaindole, with minor changes of the pyrrole ring. The resulting geometry changes are interpreted on the basis of *ab initio* calculations.

1. Introduction

Compared with the vast literature on the structures of molecules in their electronic ground states, relatively little is known about their structures in electronically excited states. This is due to the fact that standard methods for structure determination, such as X-ray or neutron diffraction or microwave spectroscopy, cannot be applied to electronically excited states. Methodical exceptions are rotationally resolved laser-induced fluorescence spectroscopy, its resonant ionization variant, and rotational coherence spectroscopy. All three methods give the inertial parameters of the investigated molecules for the ground state and the electronically excited state. For medium-sized molecules, the number of structural parameters already far exceeds the number of inertial constants. Thus, isotopic species of the parent compound have to be utilized to overcome this problem. Owing to the immense experimental effort involved, a sufficient number of different isotopomers for a complete, or nearly complete, structure determination for both electronic states has only been used in a few studies [1].

An alternative approach to the excited state structure is facilitated by the Franck–Condon (FC) principle. According to the FC principle, the probability of a vibronic transition, and thus the relative intensity of a vibronic band, depends on the overlap integral of the vibrational wave functions of both electronic states. This overlap integral is determined by the relative shift of the two potential energy curves connected by the vibronic transition along the normal coordinates Q of both states:

$$FC = \left| \int [\Psi'(Q')]^* \Psi''(Q'') \, \mathrm{d}Q' \right|^2 = \langle v' \ldots v'_N | v'' \ldots v''_N \rangle^2, \tag{1}$$

where $\Psi(Q)$ are the N-dimensional vibrational wavefunctions. The normal coordinates Q' of the excited state and Q'' of the ground state are related by the linear orthogonal transformation given by Duschinsky [2].

Thus, via the calculated FC factors, the structural change upon electronic excitation can be deduced from the experimentally determined intensity pattern. A fit of the geometry change to the observed intensity pattern requires an efficient algorithm to compute all necessary FC factors. We use the recursive relation, given by Doktorov *et al.* [3, 4], to calculate the FC factors in the harmonic approximation. Recently, we presented a program to perform fits of the intensity distributions in fluorescence emission spectra and of the changes in rotational constants of selected isotopomers [5]. In the paper, the underlying theoretical basis of the calculation of the integrals in equation (1) and the fitting procedure are presented.

Apart from the FC factor, a frequency factor has to be taken into account for calculation of the intensities of the emission lines. If the intensities of spontaneous emission lines are measured by photon counting techniques, their intensities are proportional to

*Authors for correspondence. e-mail: mschmitt@uni-duesseldorf.de/ kleinermanns@uni-duesseldorf.de

†Current address: Bruker-Daltonik GmbH, 28359 Bremen, Germany.

Molecular Physics ISSN 0026–8976 print/ISSN 1362–3028 online © 2004 Taylor & Francis Ltd
http://www.tandf.co.uk/journals
DOI: 10.1080/00268970410001725792

$\tilde{\nu}^3$,where $\tilde{\nu}$ is the experimental wavenumber of the respective transition [6]. A $\tilde{\nu}^4$ dependence of the intensities would hold if the energy of the photons was measured. Thus, all measured relative intensities were scaled using a factor of $\tilde{\nu}^3$.

7-Azaindole (7AI) has attracted considerable interest as a model system for DNA base pairs [7] and as an optical probe in proteins, replacing tryptophan [8]. Dispersed fluorescence (DF) spectra of 7AI were reported by Fuke *et al.* [9] and later by Huang *et al.* [10]. Fuke *et al.* measured the DF spectra via excitation of the electronic origin and two excited vibronic bands. Using the propensity rule, they decided which bands in the excitation spectrum and in the DF spectrum belong to the same vibrational mode. Cané *et al.* measured the gas-phase IR spectrum of 7AI in the region between 100 and 4000 cm^{-1} [11]. They gave a complete vibrational assignment, based on comparison with a scaled quantum-mechanical force field.

The structure of 7AI in different electronic states has been investigated at various levels of theory, ranging from semi-empirical methods such as INDO [12], to configuration interaction with single excitation (CIS) [13, 14], to multiconfigurational self-consistent field (MCSCF) methods such as the complete active space self-consistent field (CASSCF) [15, 16] and second-order multiconfigurational quasi-degenerate perturbation theory MCQDPT2 [17]. The ground state and lowest excited $\pi\pi^*$ state were found to be planar at all levels of theory.

In a previous paper, we determined the structure of 7AI in the electronic ground and excited state separately by rotationally resolved UV spectroscopy [18]. In the present paper we determine the geometry changes upon electronic excitation via a Franck–Condon fit of the emission line intensities from dispersed fluorescence spectra, excited through various vibronic bands, and compare the results with *ab initio* calculations.

2. Experimental

The experimental setup for the dispersed fluorescence spectroscopy is described in detail in [19, 20]. In brief, the sample was evaporated at 380 K and expanded through a pulsed nozzle with a 500 μm orifice (General Valve) into the vacuum chamber using helium as carrier gas. The output of a Nd:YAG (Spectra Physics, Quanta Ray Indi) pumped dye laser (Lambda-Physik, FL3002) was frequency doubled and crossed the molecular beam perpendicularly. The fluorescence light was collected perpendicularly to the laser and the jet and was imaged on the entrance slit of a 1 m monochromator (Jobin Yvon, grating with 2400 grooves/mm blazed at 400 nm for first order). The entrance slit was varied between 10 and 50 μm, depending on the intensity of the pumped band. The dispersed fluorescence was recorded using an intensified CCD camera (Flamestar II, LaVision). One dispersed fluorescence spectrum was obtained by summing the signal of 200 laser pulses and subtracting the background that emerges from scattered light. Twenty-five of these single spectra were summed to obtain a better signal-to-noise ratio. This allows the imaging of a DF spectrum of about 600 cm^{-1} simultaneously. Accordingly, the relative intensities in our DF spectra do not vary with laser power. Only the intensity of the excited band is perturbed by scattered light. Thus, we normalize relative intensities with respect to the strongest band in the spectrum other than the resonance fluorescence band. The intensity error of the complete detection system (including grating, CCD chip, etc.) was checked by shifting a particular fluorescence line over the CCD chip by changing the grating position. The line intensity was monitored as a function of its position on the chip. This procedure was repeated for a number of fluorescence bands. The observed intensity error was 10% at maximum.

3. Results

3.1. *Ab initio calculations*

Ab initio calculations at the complete active space self-consistent field (CASSCF) and density functional theory (DFT) levels of theory with the B3LYP functional were carried out using the Gaussian 98 program package (revision 11) [21]. The SCF convergence criterion used throughout the calculations was an energy change below 10^{-8} Hartree, and a convergence criterion for the gradient optimization of the molecular geometry of $\partial E/\partial r < 1.5 \times 10^{-5}$ Hartree/Bohr and $\partial E/\partial \varphi < 1.5 \times 10^{-5}$ Hartree/degrees, respectively. Poples 6-311G(d,p) basis set [22] was used for the DFT calculations, while the CASSCF calculations were performed using the 6-31G(d,p) basis set. The complete π space (10,9) including the *N*-lone pair with correct π symmetry was utilized as active space.

Further CASSCF calculations were performed with the MOLCAS program package (version 5.4) [23] in order to determine the orientation of the transition dipole moment. The same basis set as with Gaussian and the same active space were used. Additionally, we performed CASPT2 single-point calculations on the optimized structures. All calculations were performed on a Silicon Graphics Origin2000.

All structures are optimized using C_s symmetry constraints, because the experimental results of Schmitt *et al.* showed that 7-azaindole is planar in the S_0 and S_1 states [18]. The structure of 7AI was optimized at the B3LYP/6-311G(d,p) and CASSCF/6-31G(d,p) levels of theory and the harmonic vibrational frequencies were calculated using the analytical second

Table 1. S_0 state geometry parameters calculated at the B3LYP/6-311G(d,p) and CASSCF/6-31G(d,p) levels of theory. The atomic numbering refers to figure 1.

S_0	B3LYP	CAS(10,9)	Exp.[a]
A''	3945	3973	3928.93
B''	1702	1708	1702.629
C''	1189	1195	1188.128
N1–C2	138.10	137.70	
C2–C3	136.90	136.50	
C3–C3a	143.40	144.10	
C3a–C7a	142.40	141.00	
C7a–N1	137.50	136.60	
C3a–C4	139.90	140.00	
C4–C5	138.90	138.90	
C5–C6	140.50	140.60	
C6–N7	133.50	132.90	
N7–C7a	132.80	132.60	
N1–H	100.70	99.20	
C2–H	107.90	107.00	
C3–H	107.90	107.10	
C4–H	108.50	107.60	
C5–H	108.30	107.50	
C6–H	108.60	107.60	

[a]From [18].

derivatives. The resulting geometry parameters and rotational constants are presented in table 1. The atomic numbering in table 2 refers to figure 1. The B3LYP calculation performs very well with respect to the rotational constants. The largest deviation from the experimentally determined rotational constants is less than 0.5%. However, the CASSCF calculation also results in a very reliable geometry, with deviations of the rotational constants of less than 1%. This is crucial for the utilization of the ground-state geometry as a basis for the displacements along the normal coordinates in the FC fit (*vide infra*).

Table 2 presents the vibrational frequencies of the 39 normal modes of 7AI calculated at the B3LYP/6-311G(d,p) level of theory. The irreducible representation of nuclear motion in the C_s point group transforms as $\Gamma_{nuc} = 30a' + 15a''$. Translations and rotations are represented by the transformations $\Gamma_{trans} = 2a' + a''$ and $\Gamma_{rot} = a' + 2a''$, which leads to symmetries of the 39 normal modes of $27a' + 12a''$. The vibrations shown in table 2 are sorted with the 27 in-plane motions in ascending frequency, followed by the 12 out-of-plane vibrations. The electronically excited $\tilde{A}^1$ state is of A′ symmetry. Therefore, only in-plane a' vibrations are allowed, because the transition dipole moment of the $\pi\pi^*$ transition is located in the molecular plane. Out-of-plane a'' motions appear as overtones in the respective spectra.

The numbering of the modes follows the nomenclature of Varsanyi [24] for *ortho*-di-light-substituted benzene derivatives, complete with vibrations of the five-membered ring [20]. As 7AI is rather an unsymmetrical molecule, the numbering scheme is not always unique and has to be taken as a rough description of the mode. The respective vibration should be inspected as an animated graph using a viewer such as Molden [25] or Molekel [26]. The Gaussian .log file, which contains the normal mode analysis, can be downloaded from our home page (http://www-public.rz.uni-duesseldorf.de/126pc1). The quoted calculated frequencies are unscaled and are compared with the experimental frequencies in table 2. In the region between 1350 and 1550 cm^{-1} and in the range of the CH stretching vibrations, the spectra are too dense to allow a straightforward vibrational assignment.

The vertical and adiabatic excitation energies for the two lowest $\pi\pi^*$ transitions have been calculated at the CASSCF(10,9)/6-31G(d,p) and CASPT2(10,9)/6-31G(d,p) levels using CAS optimized structures. Table 3 reports the excitation energies, oscillator strengths and directions of the transition dipole moments for both transitions.

The experimentally determined vibrationless electronic origin (^1L_b) of 7AI is at 34 630.74 cm^{-1} (414 kJ/mol, 4.29 eV), in good agreement with the adiabatic CASPT2(10,9)/6-31G(d,p) transition energy of 33 683 cm^{-1} (402 kJ/mol, 4.18 eV). The transition to the next $\pi\pi^*$ state (^1L_a) is calculated to be only 1500 cm^{-1} (18 kJ/mol, 0.18 eV) higher in energy.

The CAS orbitals that are involved in the two lowest $\pi\pi^*$ transitions are shown in figure 2. Their shape differs considerably from the CIS orbitals shown in figure 7 of [18] due to the optimization of the MO coefficients in the CAS calculations. The squares (weights) of the CI coefficients of the excitations to ^1L_b and ^1L_a are depicted in Figure 2. The transition to ^1L_b has large contributions from excitations from orbitals 30 to 32 (weight 0.55) and from orbitals 31 to 33 (weight 0.20). The dominant excitation of the ^1L_a state takes place from orbital 31 to 32 (weight 0.75).

3.2. *Excitation and emission spectra*

Figure 3 shows the fluorescence excitation spectrum of 7AI in the region between 34 600 and 36 300 cm^{-1}. The bands marked with an asterisk were excited to obtain the DF spectra that are shown in figures 4 and 5. The assignment of these absorption bands to specific vibrational motions in the excited state was made on the basis of the propensity rule from the intensities in the emission spectra and is given in the inset of figure 3. The assignment will be explained below, together with a discussion of the respective ground-state vibrations.

Table 2. B3LYP/6-311G(d,p) calculated ground-state vibrational frequencies and description of the motions. All frequencies are given in cm^{-1}. The numbering follows the nomenclature of Varsanyi [24] for *ortho*-di-light-substituted benzene derivatives, completed for vibrations of the five-membered ring [20]. In-plane vibrations (a') are on the left and out-of-plane vibrations (a'') are on the right.

Assignment	Calc.	Obs.	Obs. calc	Assignment	Calc.	Obs.[a]	Obs. calc
9b	431	434	1.01	10a	223	459	1.03
6a	562	562	1.00	10b	245	478	0.98
6b	636	642	1.01	NH(inv.)	428	847	1.00
1	775	769	0.98	4a	482		–
12a	901	899	0.99	4b	598		–
12b	912	908	0.99	16a	622		–
18b	1057	1044	0.99	CH(inv.)	731		–
δCH	1085	1075	0.99	11	792		–
δCH	1106	1114	1.01	17a	818		–
18a	1136	1141	1.00	CH(inv.)	872		–
9a	1221	1220	1.00	5	947		–
3	1270	1293	1.02	17b	979		–
δNH	1312	1307	1.00				
δNH	1346	1358	1.01				
δCH	1369	–	–				
19b	1439	–	–				
δNHδCH	1451						
19a	1526	–	–				
δNHδCH	1538	–	–				
8a	1616	1612	1.00				
8b	1642	1634	1.00				
νCH	3151	–	–				
νCH	3169	–	–				
νCH	3191	–	–				
νCH	3236						
νCH	3256	–	–				
νNH	3666	–	–				

[a]First overtones.

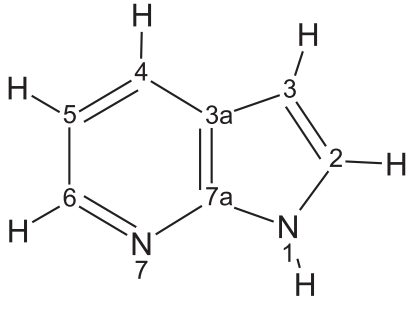

1*H*-pyrrolo[2,3-*b*]pyridine

Figure 1. Atomic numbering of 7AI.

Table 3. Vertical and adiabatic excitation energies (in cm^{-1}), oscillator strengths (in $bohr^2 \cdot$ hartree) and orientation of the transition dipole moments (in degrees) for the two lowest ππ* transitions.

	CASSCF(10,9)		
	Vertical	Adiabatic	TDM
$S_1(^1L_b) \leftarrow S_0$	38 739	37 622	+29.9°
$S_2(^1L_a) \leftarrow S_0$	47 687	44 767	−33.5°
	CASPT2(10,9)		Osc. strength
$S_1(^1L_b) \leftarrow S_0$	35 758	33 683	0.049
$S_2(^1L_a) \leftarrow S_0$	39 661	35 208	0.069

The first trace (a) of figure 4 shows the fluorescence emission spectrum, obtained via excitation of the vibrationless origin 0,0. The assignments given in figures 4 and 5 are based on the *ab initio* calculations described in Section 3.1. The calculated frequencies for the ground-state vibrations that were used for the assignment are summarized in table 4.

The strongest band in the emission spectrum after excitation at $0,0 + 233\,cm^{-1}$ (trace d of figure 4) is found at $432.5\,cm^{-1}$ and can be assigned on the basis of B3LYP/6-311G(d,p) calculations to the 9b vibration. The corresponding computed frequency value from the B3LYP calculation is quite close ($431\,cm^{-1}$) (see table 4).

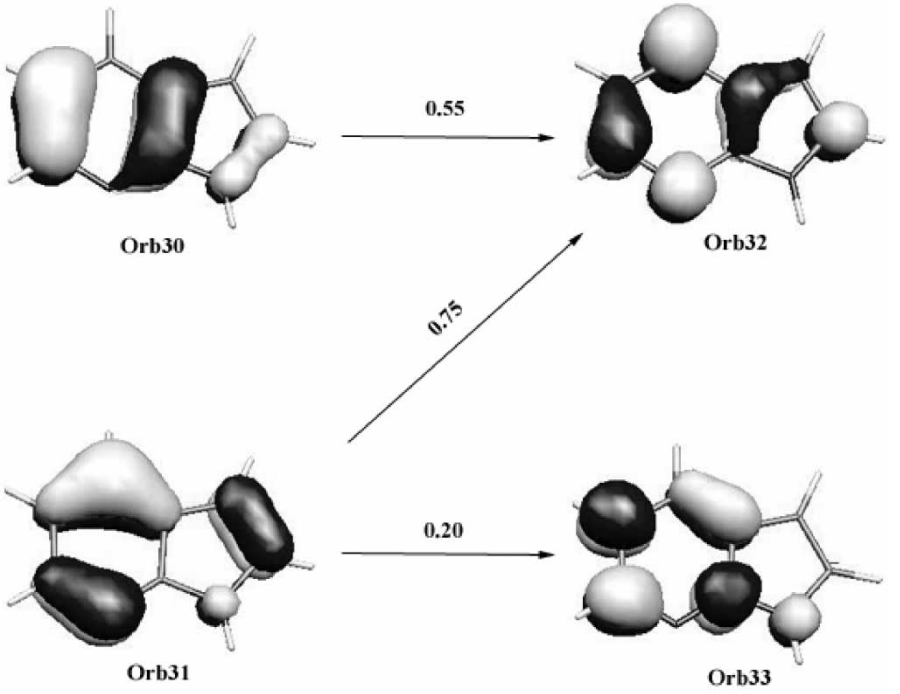

Figure 2. Weights of the CAS molecular orbitals that are involved in the two lowest $\pi\pi^*$ transitions. The orbitals are ordered by their HF energy.

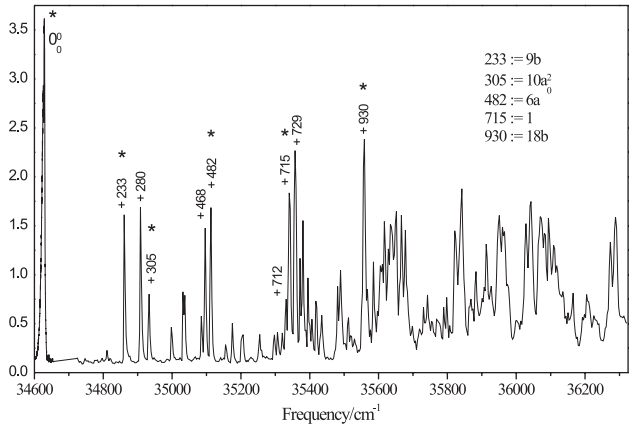

Figure 3. Fluorescence excitation spectrum of 7AI in the region between 34 600 and 36 300 cm^{-1}.

The 9b vibration can be described as an in-plane rotational motion of both rings against each other. Also, the overtone and combination bands of this mode with 6a and 6b are observed. The assignment of the 233 cm^{-1} band in the absorption spectrum to 9b in the S_1 state therefore appears reasonable.

Upon excitation of 0,0+305 cm^{-1} the emission spectrum shows a progression and combination with a band at 459 cm^{-1} (trace g of figure 4). Comparison with the results of the B3LYP calculations shows that this mode can be assigned to the overtone of mode 10a in the harmonic approximation. This mode is a concerted out-of-plane motion of both rings about the central C3a–C7a bond and therefore is only allowed as the first overtone for a planar molecule. Also in this case, the propensity rule allows for an unequivocal assignment of the transition at 305 cm^{-1} to the overtone of this 'butterfly mode' in the S_1 state.

Excitation at 482 cm^{-1} (first trace of figure 5) results in a long progression up to the third overtone of a band at 562 cm^{-1} and combination bands of this vibration with various other in-plane modes in the emission spectrum. The B3LYP calculations allow a straightforward assignment of the S_1 vibration at 482 cm^{-1} to mode 6a.

Excitation at 715 cm^{-1} (trace d of figure 5) gives a clear indication in the emission spectra that mode 1 is excited. The strongest band in the emission spectrum at 1550 cm^{-1} can be assigned to the first overtone of vibration 1, and appears as a long progression. The B3LYP calculated frequency for this band is 775 cm^{-1} and shows good agreement in the harmonic approximation with the experimentally determined frequency.

The band at 930 cm^{-1} above the electronic origin in the fluorescence excitation spectrum is assigned to a vibration with a frequency of 1044 cm^{-1} from the progression in the emission spectrum (trace g of figure 5). Comparison with the B3LYP calculations shows that this vibration at 1044 cm^{-1} has to be assigned to mode 18b (B3LYP: 1057 cm^{-1}).

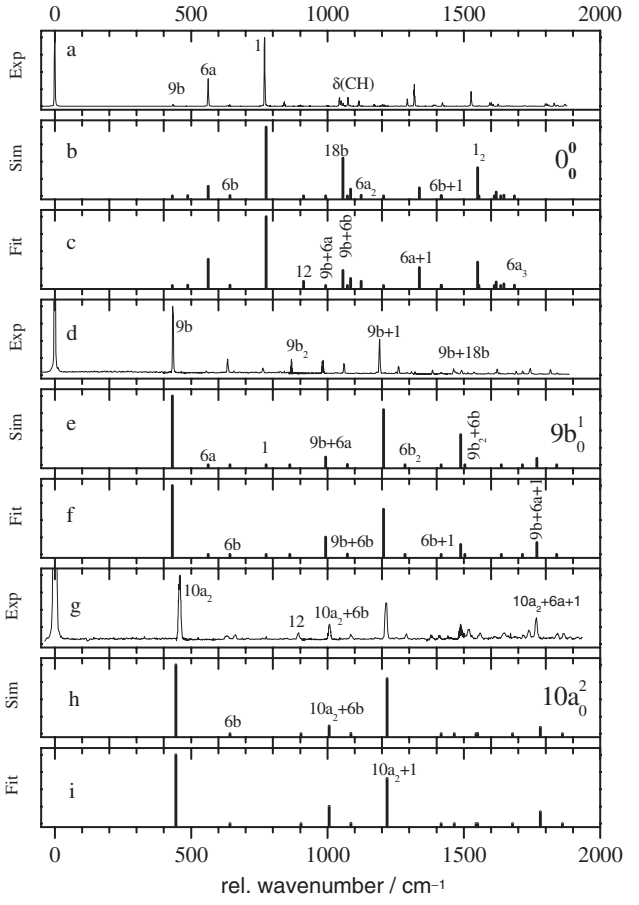

Figure 4. Fluorescence emission spectra of 7AI pumped via 0,0, $0,0+233\,cm^{-1}$ and $0,0+305\,cm^{-1}$.

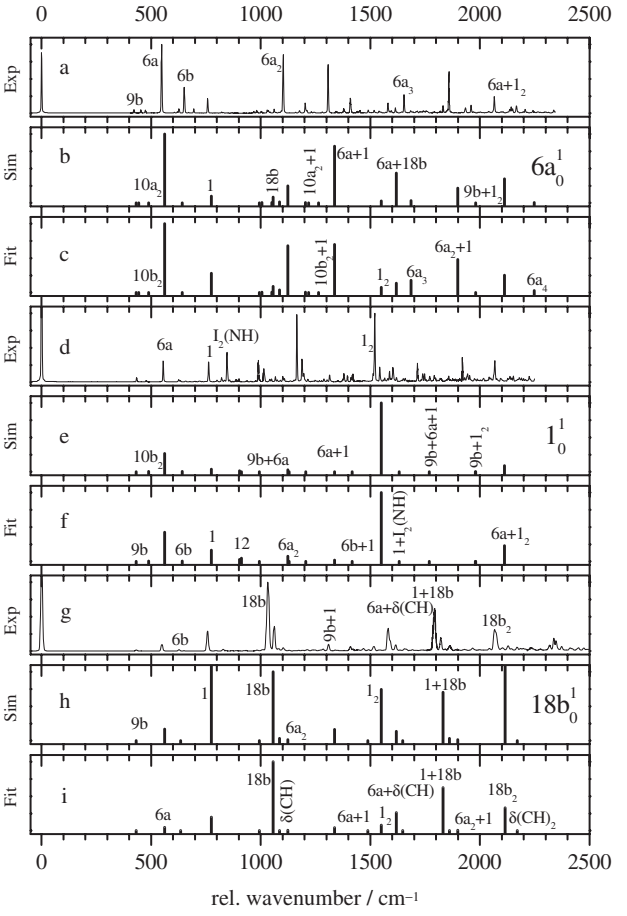

Figure 5. Fluorescence emission spectra of 7AI pumped via $0,0+482\,cm^{-1}$, $0,0+715\,cm^{-1}$ and $0,0+930\,cm^{-1}$.

The intensities of the emission bands after excitation of the described S_1 state vibrations are summarized in table 5. They show clearly how the strongest transition (marked by an asterisk) appears upon excitation of the corresponding vibration in the excited state, illustrating the propensity rule.

3.3. *Determination of the structure*

The change in molecular geometry upon electronic excitation can be determined from the intensities of the absorption or emission bands using the FC principle. The fit procedure has been explained in detail in a previous publication [5]. In a first step the geometry and Hessian matrix of both the ground and excited state are calculated at the CASSCF(10,9)/6-31G(d,p) level. Using the recursion formula given by Doktorov [3, 4] the Franck–Condon factors of the observed and assigned transitions are calculated and a simulated intensity distribution is obtained. In subsequent steps, the S_1 state geometry is displaced along selected normal coordinates and the resulting intensity pattern is calculated. The displacements are iterated until the observed intensity pattern matches the simulated pattern. If experimental data for rotational constants in both states are available (possibly for several isotopomers), their changes upon electronic excitation can be used as an additional part of the overall FC fit. The fit was performed using the program *FCFit*, which was developed by our group and has been described previously [5]. The use of a selected sub-ensemble of normal modes as the basis for the displacements is forced by the difficulty in assigning a sufficient number of vibrations in the electronically excited state. This selection has to be performed carefully, in order to avoid artificial displacement effects by consideration of modes that are too similar.

Emission spectra have been obtained from excitation of 0,0, 9b, $10a_2^0$, 6a, 1 and 18b. The intensities of vibration 10a ('butterfly mode') in the emission spectra were not used for the FC fit, because 7AI is known to be planar in both electronic states. Additionally, the intensity of the CH bending mode, δ(CH), was included in the fit. This mode shows up in the emission spectrum upon excitation of the electronic origin, the 6a vibration and the 18b vibration. Thus, the six motions which form

the basis for the displacements upon electronic excitation are 9b, 6a, 1, 12, 18b and δ(CH). All are in-plane modes and are depicted in figure 6.

First, a simulation of the intensities of the emission bands was performed using the geometries and the Hessian matrices from the CASSCF(10,9)/6-31G(d,p) calculations. These simulations are shown in the traces which follow the respective experimental emission spectrum in figures 4 and 5. Although the overall performance of these simulations does not seem to be too bad, there are severe deviations between the experimental and simulated intensities. In the emission spectrum via excitation of 0,0, the intensity of mode 6a is underestimated, whereas the intensity of mode 18b is strongly overestimated. The largest deviations are observed for the spectrum obtained after excitation of mode 18b. In the simulation the intensities of modes 1 and $18b_2$ are strongly overestimated. Both bands are more intensive in the simulation than the pumped band 18b. The experimental trace, however, shows a completely different situation, with very weak 1 and $18b_2$ bands and 18b as the strongest transition.

Table 4. Experimental and calculated ground-state vibrational frequencies and assignments of the motions. All frequencies are given in cm^{-1}.

Exp.	B3LYP	Assignment	Exp.	B3LYP	Assignment
434	431	9b	1220	1221	$10a_2^0+1$
459	446	$10a_2^0$	1242	1264	$10b_2^0+1$
478	489	$10b_2^0$	1261	1272	$6b_2^0$
562	562	6a	1319	1337	6a + 1
642	636	6b	1396	1411	6b + 1
769	775	1	1422	1463	6a + 12a
847	856	$NH(inv.)_2^0$	1445	1488	9b + 18b
868	862	$9b_2^0$	1463	1550	1_2^0
899	901	12a	1527	1537	6b + 12a
998	993	9b + 6a	1560	1619	6a + 18b
1008	1008	$10a_2^0+6a$	1607	1647	$6a+\delta(CH)$
1038	1051	$10b_2^0+6a$	1612	1616	8a
1044	1057	18b	1634	1642	8b
1057	1067	9b + 6b	1647	1686	$6a_3^0$
1075	1085	$\delta(CH)$	1666	1832	1 + 18b
1086	1082	$10a_2^0+6b$	1805	1860	$1+\delta(CH)$
1114	1124	$6a_2^0$	1835	2114	$18b_2^0$
1185	1198	6a + 6b	2084	2170	$\delta(CH)_2^0$
1202	1206	9b + 1	2140	2248	$6a_4^0$

After the simulations with unchanged geometries, we performed FC fits of the intensities of the vibrations, overtones and combination bands in the spectra of figures 4 and 5 by displacing the S_1 state geometry along the six normal modes described above. The results are shown in the traces that follow the respective FC simulations in figures 4 and 5. Close inspection of all emission spectra shows that the intensity pattern is well reproduced upon displacement of the S_1 geometry. As a representative example, let us compare the experimental spectrum, the simulation and the fit of the emission spectrum upon 18b excitation (figure 5, traces g, h and i). The intensity of mode 6a is slightly too large in the simulation, but is corrected in the fit. The most obvious improvement is in the intensity of mode 1. In the simulation, this band is the strongest, although it is quite weak in the experimental spectrum. Also, the quality of the simulation of the 18b progression is quite bad. The experimental spectrum shows a rapid decline of overtone intensities, whereas, in the simulation, the first overtone of the 18b mode is calculated to be the strongest. The coupling to mode 1 is strongly exaggerated, therefore the intensity of the combination band 1 + 18b is also different from the experimental value. All of these intensities are very well reproduced in the FC fit of the 18b emission spectrum (see figure 5, trace i).

Table 6 shows the results for the S_1 displacement obtained from the Franck–Condon fit described above. The first column gives the results for the geometry change upon electronic excitation as obtained from

Table 5. Intensities of emission bands relative to the most intense band of the respective spectrum (not including the resonance fluorescence band) after excitation of different S_1 vibrations. The transition marked with an asterisk is the strongest transition in the respective emission spectrum and is utilized to identify the S_1 mode used for excitation.

	S_1 state transition					
	0,0	0,0 + 233	0,0 + 305	0,0 + 482	0,0 + 715	0,0 + 930
9b	0.0267	1.0000*	0.0000	0.0484	0.0670	0.0138
$10a_2^0$	0.0000	0.0000	1.0000*	0.0507	0.0000	0.0000
6a	0.3990	0.0627	0.0000	1.0000*	0.3059	0.0929
1	1.0000	0.1024	0.0000	0.2149	0.2919*	0.2904
1_2^0	0.2144	0.0439	0.2851	0.0416	1.0000*	0.0667
12	0.0198	0.0000	0.1606	0.0000	0.0338	0.0000
18b	0.1235	0.0000	0.0000	0.0406	0.0413	1.0000*
δ(CH)	0.1183	0.0000	0.0000	0.0592	0.0780	0.3787

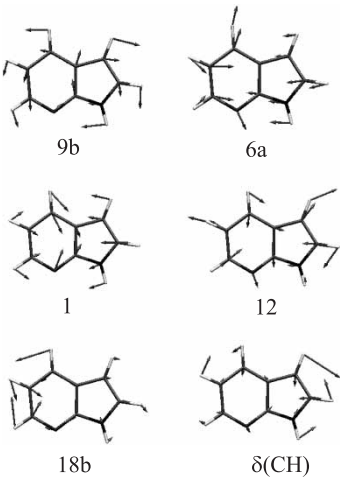

Figure 6. Normal modes used as the basis for the structure fit in the electronically excited state.

Table 6. Comparison of the changes in geometry upon electronic excitation from a CASSCF(10/9) study, from the Franck–Condon fit described in the text, and from a structure fit to rotational constants (r_0) from [18]. All bond length changes are given in pm, bond angle changes in degrees.

	CAS(10,9)	FC fit	r_0
Bond length			
N1–C2	+1.3	+1.2	+2.0
C2–C3	+1.5	+1.6	−3.8
C3–C3a	−1.5	−1.2	−2.3
C3a–C7a	+4.5	+4.7	+2.8
C7a–N1	−0.8	−1.6	+2.0
C3a–C4	+2.0	+1.9	+1.1
C4–C5	+5.0	+3.8	+1.1
C5–C6	+3.6	+2.3	+2.8
C6–N7	+3.5	+3.0	±0
N7–C7a	+1.4	+1.2	+4.0
Five ring (mean)	+1.0	+0.94	+0.14
Six ring (mean)	+3.3	+2.8	+2.46
Angle			
N1–C2–C3	−1.3	−0.8	
C2–C3–C3a	+1.2	+0.4	
C3–C3a–C7a	−0.24	+0.2	
C3a–C7a–N1	−1.2	−1.4	
C7a–N1–C2	+1.6	+1.7	
C3a–C4–C5	−2.7	−2.5	
C4–C5–C6	+1.4	+1.0	
C5–C6–N7	+0.5	+2.0	
C6–N7–C7a	−2.1	−3.4	
N7–C7a–C3a	+1.8	+2.2	
C7a–C3a–C4	+1.1	+0.7	

the CASSCF calculations. The second column presents the results for the geometry changes from the Franck–Condon fit to 107 fluorescence emission bands and to the changes in the rotational constants of four isotopomers

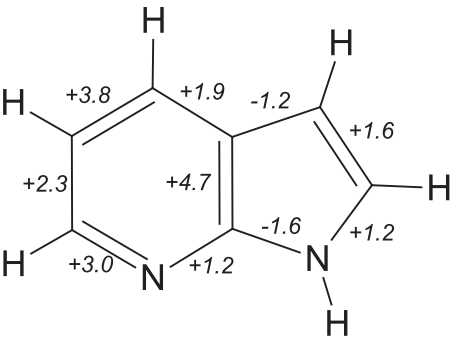

Figure 7. Schematic drawing of the changes in geometry of 7AI upon electronic excitation. All bond length changes are given in pm. The respective changes in bond angles are given in table 6.

of 7AI, taken from the first publication of this series [18]. These isotopomers are the normal isotopomer (i) 1*H*-pyrrolo(2,3-*b*)pyridine (7AI), (ii) 1*H*-pyrrolo[2,3-*b*]pyridine-1-d_1, (iii) 1*H*-pyrrolo[2,3-*b*] pyridine-3-d_1, and (iv) 1*H*-pyrrolo[2,3-*b*]pyridine-1,3-d_2 (see figure 1 of [18] for the substitution positions). The last column gives the results for a direct structure fit to the above isotopomers for comparison, which was performed in the first paper of this series [18].

4. Conclusions

The changes in geometry of 7AI upon electronic excitation are summarized in figure 7. The change in the 7AI geometry can be described as an overall expansion of the pyridine moiety, with smaller effects in the pyrrole ring. These findings are very similar to the results of a preceding study in which the structure was determined from the rotational constants of both states. Some remarks are needed with respect to the structure determined from the FC analysis: the DF spectra were recorded upon excitation of vibronic levels within 1000 cm^{-1} of the electronic origin. These are all ring-deformation vibrations. No CH or NH vibrations were excited. Thus, from a pure FC analysis, the structural changes are only sensitive to ring deformations. Nevertheless, the rotational constants of the isotopically excited species also allow the determination of deformations other than just ring deformations.

Both methods agree that the sum of the changes of all bond lengths in the pyridine ring is larger than in the pyrrole ring (see table 6). Nevertheless, there are differences that need to be addressed. Especially for the C2–C3 bond in the pyrrole moiety, the FC fit finds an increase in the bond length, whereas from the fit to the rotational constants, a decrease of the respective bond length is predicted. As both methods have their peculiar discrepancies, the question concerning this change in bond length has to be left open until more experimental data become available. The fit to a r_0

structure, as performed in [18], neglects the different zero-point energy (ZPE) contributions of the different isotopomers. Furthermore, due to the limited number of isotopomers, some constraints to the model geometry had to be made, which confine the validity of the determination of the structural changes. These problems can be overcome by measurement of the rotationally resolved spectra of more isotopomers, preferably substituted at the questionable positions C2 and C3. On the other hand, the FC fit restricts the possible geometry changes by selecting a sub-ensemble from the $3N-6$ normal modes that form the complete basis for the distortion along the normal coordinates. Additionally, the changes in the rotational constant are related to the geometry of the vibrational ground state of the electronic ground state. In the FC fit, the resulting geometry is vibrationally averaged over several vibronic states. These differences will be much larger than the differences due to the ZPE contributions to the vibrational origins of the different isotopomers (*vide supra*).

As can be seen from figure 2, the main effects of electronic excitation to the ^1L_b state take place in the pyridine ring, with smaller contributions in the pyrrole moiety. The effects in the pyridine ring are more obvious. The two main excitations to the ^1L_b state both transfer electron density from bonding to non-bonding orbitals, thus reducing the overall bond order in the six-membered ring, as observed in the experiment. The situation in the five-membered ring is more complex: the excitations are of the type non-bonding $\rightarrow$ anti-bonding and bonding $\rightarrow$ non-bonding and should lead to a smaller decrease of the bond order and therefore to a smaller ring expansion. This general tendency is supported by both the Franck–Condon fit and the r_0 structure fit.

The financial support of the Deutsche Forschungsgemeinschaft (KL531/22-1) is gratefully acknowledged. We thank W. L. Meerts for helpful discussions. This work forms part of the PhD thesis of Robert Brause.

References

[1] Ratzer, C., Küpper, J., Spangenberg, D., and Schmitt, M., 2002, *Chem. Phys.*, **283,** 153.
[2] Duschinsky, F., 1937, *Acta Physicochim. URSS*, **7,** 551.
[3] Doktorov, E. V., Malkin, I. A., and Man'ko, V. I., 1975, *J. Molec. Spectrosc.*, **56,** 1.
[4] Doktorov, E. V., Malkin, I. A., and Man'ko, V. I., 1977, *J. Molec. Specrosc.*, **64,** 302.
[5] Spangenberg, D., Imhof, P., and Kleinermanns, K., 2003, *Phys. Chem. chem. Phys.*, **5,** 2505.
[6] Roy, R. J. L., 1998, *J. Molec. Spectrosc.*, **192,** 237.
[7] Kasha, M., Horowitz, P., and El-Bayoumi, M. A., 1972, *Molecular Spectroscopy: Modern Research*, vol. I (New York: Academic Press), p. 287.
[8] Smirnow, A. V., English, D. S., Rich, R. L., Lane, J., Teyton, L., Schwabacher, A. W., Luo, S., Thornburg, R. W., and Petrich, J. W., 1997, *J. phys. Chem.* B, **101,** 2758.
[9] Fuke, K., Yoshiuchi, H., Kaya, K., Achiba, Y., Sato, K., and Kimura, K., 1984, *J. phys. Chem.*, **88,** 5840.
[10] Huang, Y., Arnold, S., and Sulkes, M., 1996, *J. phys. Chem.*, **100,** 4734.
[11] Cané, E., Palmieri, P., Tarroni, R., and Trombetti, A., 1994, *J. Chem. Soc., Faraday Trans.*, **90,** 3213.
[12] Ilich, P., 1995, *J. Molec. Struct.*, **354,** 37.
[13] Shukla, M. K., and Mishra, P. C., 1998, *Chem. Phys.*, **230,** 187.
[14] Graña, A. M., 1999, *J. Molec. Struct. Theochem*, **466,** 145.
[15] Borin, A. C., and Serrano-Andrés, L., 2000, *Chem. Phys.*, **262,** 253.
[16] Luis Serrano-Andrés, A. C. B., 2000, *Chem. Phys.*, **262,** 267.
[17] Chaban, G. M., and Gordon, M. S., 1999, *J. phys. Chem.* A, **103,** 185.
[18] Schmitt, M., Ratzer, C., Kleinermanns, K., and Meerts, W. L., 2004, *Molec. Phys.*, **102,** 1605.
[19] Schmitt, M., Henrichs, U., Müller, H., and Kleinermanns, K., 1995, *J. chem. Phys.*, **103,** 9918.
[20] Roth, W., Jacoby, C., Westphal, A., and Schmitt, M., 1998, *J. phys. Chem.* A, **102,** 3048.
[21] Frisch, M. J., Trucks, G. W., Schlegel, H. B., Scuseria, G. E., Robb, M. A., Cheeseman, J. R., Zakrzewski, V. G., Montgomery, J. A., Jr., Stratmann, R. E., Burant, J. C., Dapprich, S., Millam, J. M., Daniels, A. D., Kudin, K. N., Strain, M. C., Farkas, O., Tomasi, J., Barone, V., Cossi, M., Cammi, R., Mennucci, B., Pomelli, C., Adamo, C., Clifford, S., Ochterski, J., Petersson, G. A., Ayala, P. Y., Cui, Q., Morokuma, K., Salvador, P., Dannenberg, J. J., Malick, D. K., Rabuck, A. D., Raghavachari, K., Foresman, J. B., Cioslowski, J., Ortiz, J. V., Baboul, A. G., Stefanov, B. B., Liu, G., Liashenko, A., Piskorz, P., Komaromi, I., Gomperts, R., Martin, R. L., Fox, D. J., Keith, T., Al-Laham, M. A., Peng, C. Y., Nanayakkara, A., Challacombe, M., Gill, P. M. W., Johnson, B., Chen, W., Wong, M. W., Andres, J., Gonzalez, C., Head-Gordon, M., Replogle, E. S., and Pople, J. A., 2001, Gaussian 98, revision a.11 (Pittsburgh, PA: Gaussian, Inc.).
[22] Krishnan, J. S., and Binkley, R. S. J. P., 1980, *J. chem. Phys.*, **72,** 650.
[23] Andersson, K., Barysz, M., Bernhardsson, A., Blomberg, M. R. A., Cooper, D. L., Fülscher, M. P., de Graaf, C., Hess, B. A., Karlström, G., Lindh, R., Malmqvist, P.-A., Nakajima, T., Neogrády, P., Olsen, J., Roos, B. O., Schimmelpfennig, B., Schütz, M., Seijo, L., Serrano-Andrés, L., Siegbahn, P. E. M., Stalring, J., Thorsteinsson, T., Veryazov, V., and Widmark, P.-O., 2002, Molcas Version 5.4, Lund University, Sweden.
[24] Varsanyi, G., 1974, *Assignments for Vibrational Spectra of 700 Benzene Derivatives* (New York: Wiley).
[25] Schaftenaar, G., and Noordik, J., 2000, *J. Comput.-Aided Molec. Design*, **14,** 123.
[26] Portmann, S., 2002, Molekel available from the web at http://www.cscs.ch/molekel